Journal of Technology Research (JTR)
Volume 3, Issue 2, (2025), pp 133-138, ISSN 3005-639X

Synthesis and Characterization of Chromium Doped Alumina Nanoparticles

Jamal M. Aldabib* [1]

[1]Department of Dental Technology, Faculty of Medical Technology, Baniwaleed University, Baniwalid, Libya.
*Corresponding author email: jamalald71@gmail.com

Received: 25-10-2025 Accepted: 13-12-2025| Available online:18-12-2025 | DOI:10.26629/jtr.2025.16

ABSTRACT

Fine powders of chromium doped alumina were prepared by employing combustion method. The materials used in the reaction are aluminum nitrate (oxidizer), sugar (fuel) and ammonium dichromate (catalyst). The currant study was aimed to study the effect of sintering temperature on the formation of chromium doped alumina. The powder samples were sintered at three different temperatures; 900, 1000 and 11000C. Various characterization methods have been used in order to analyze the powder characteristics such as DTA, XRD, SEM and FTIR. To investigate the phases exist in the samples, X-ray diffraction (XRD) was carried out, while the morphology of the samples was investigated using a Field Emission Scanning Electron Microscope (FESEM). Finally, to investigate the types of bonding in the sample, Fourier Transform Infra-Red (FTIR) analysis was carried out. Within the limitation of the current study, the sintering temperature is considered the key criteria in the formation of chromium doped alumina. Moreover, the formation of chromium doped alumina phases is fully achieved at higher sintering temperature. Higher temperatures promote the formation of the desired, stable alumina phase and the full incorporation of chromium ions into the crystal lattice.

Keywords: Chrome doped alumina nanoparticles, Material characterization, Combustion method.

تصنيع وتوصيف جسيمات الألومينا النانوية المشبعة بالكروم

جمال امعمر الدبيب

قسم تقنية الأسنان ، كلية التقنية الطبية ، جامعة بني وليد ، بني وليد، ليبيا.

ملخـــــص البحـــــث

تم تحضير مساحيق ناعمة من الألومينا المطعّمة بالكروم باستخدام طريقة الاحتراق. شملت المواد الداخلة في التفاعل نترات الألومنيوم بوصفها مادة مؤكسِدة، والسكر كوقود، وثنائي كرومات الأمونيوم كمحفّز. هدفت الدراسة الحالية إلى بحث تأثير درجة حرارة التلبيد في تكوين الألومينا المطعّمة بالكروم. تم تلبيد عينات المسحوق عند ثلاث درجات حرارة مختلفة هي 900 و1000 و1100 درجة مئوية. استُخدمت تقنيات (XRD, SEM, FTIR) لدراسة خصائص المساحيق، مورفولوجية العينات والتعرف على أنواع الروابط الكيميائية. ضمن حدود هذه الدراسة، تُعد درجة حرارة التلبيد العامل الحاسم في تكوين الألومينا المطعّمة بالكروم. كما أظهرت النتائج أن تكوّن أطوار الألومينا المطعّمة بالكروم يكتمل عند درجات التلبيد المرتفعة، حيث تسهم درجات الحرارة الأعلى في تعزيز تكوّن طور الألومينا المستقر المطلوب وتحقيق الإدماج الكامل لأيونات الكروم داخل الشبكة البلورية.

الكلمات الدالة :جسيمات الألومينا النانوية المطعّمة بالكروم، توصيف المواد، طريقة الاحتراق.

1. INTRODUCTION

Nanoparticles are defined as particulate dispersions or solid particles with a size in the range of 10 to 1000nm[1, 2]. Materials show different properties at nanoscale compared to their bulk counterparts where their optical, chemical activities, electrical and structural activities are altered making them suitable in the application of sensing, high strength materials, catalyst and electroceramics[3, 4]. At the same time, this alteration of properties causing in complication of the characterization process[5-7]. The properties of nano-materials could be affected by several factors such as grain boundary structures and size[5, 8]. The nano-materials have great potential in wide application prospects in different industries as a function of their superior and exceptional mechanical performance [9, 10]. Nano-materials are used widely in different biomedical applications[11-13].

They have great potential in tissue engineering applications, medical sensors, drug delivery and medical X-rays[14]. Effectiveness of nano-materials in bio-medical applications is due to the small particle size and therefore large surface area[15-17]. There are various methods to produce nanoparticles such as sol-gel, vapor-phase reaction, precipitation, combustion and etc. In this analysis, combustion method was used to produce Chromium doped alumina nanoparticles. Chromium has great potential in resisting corrosion and scratches over the objects. In addition, chromium serves as a protective barrier for alumina, shielding it against corrosion, wear, and tear. It is a process that not only augments the lifespan of alumina but also improves their resistance to harsh environmental factors. Understanding the effect of sintering temperature could lead to the production of materials with superior characteristics properties. Chromium doped alumina nanoparticles offer significant advantages over other materials primarily through their unique photoluminescence (PL) properties, making them superior for applications in bio-imaging, solid-state lasers, and high-dose dosimetry[18]. They also exhibit exceptional thermo-chromic (color-changing) behaviour and enhanced mechanical strength compared to pure alumina or certain other ceramics[19]. Sintering temperature significantly influences the phase formation, crystallinity, particle size, and optical properties (color and luminescence intensity) of chromium-doped alumina nanoparticles[20]. Therefore, the current study was designed to investigate the effect of sintering temperature on the formation of chromium doped alumina.

2. MATERIALS AND METHODS

14.71g of aluminum nitrate (Sigma Aldrich, USA) and 12.86g of sugar are each weighed into 100ml beaker. Some amount of distilled water is added just enough to dissolve the salt separately. The two solutions are then mixed together into a 1 litter beaker. 0.1g of ammonium dichromate is dissolved into the mixture. The mixture is heated at 195°C on the hotplate until a dry and solid foam residue is obtained. This took approximately 1 hour. The residue is left to cool, forming some foam. The foam is ground into fine powdery form using agate mortar and pestle. The powder is divided into 3 portions and the powder samples are heated in a furnace at temperatures of 900°C, 1000°C and 1100°C respectively with a holding time of 5 hours.

Four characterization techniques, known as X-Ray Diffraction (XRD), Field Emission Scanning Electron Microscope (FESEM), Fourier Transform Infra-Red (FTIR) and Thermal Analysis have been employed in order to investigate the properties of the produced powder. To study the phases formed in the samples, XRD scans are carried out using Bruker AXS spectrometer. The angle of measurement starts from 10 to 90°. FESEM (ZEISS SupraTM, 35VP) was carried out to study the surface morphology changes of the

powder. Finally, FTIR (Perkin-Elmer) was performed to investigate the types of the bonding formed in the samples. The flow chart of samples preparation and characterization is shown in Fig. 1.

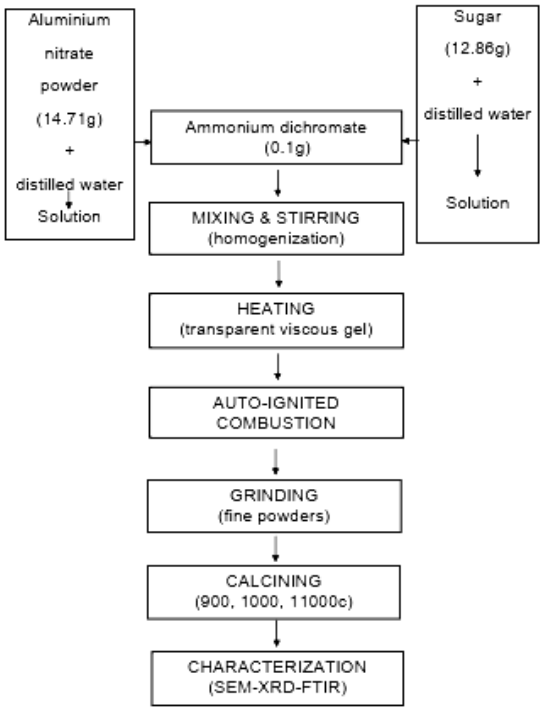

Fig 1. Flow chart for the sample's preparation and characterization.

3. RESULTS AND DISCUSSION

3.1 X-Ray Diffraction (XRD)

Fig. 2 illustrates X-ray diffraction patterns of chromium doped-alumina sintered at different temperatures (i.e., 900°C, 1000°C and 1100°C). It was observed that at low temperature (900°C), most of the peaks of chromium and alumina are hardly matched with the standard peaks of Joint Committee on Powder Diffraction Standards (JCPDS) for chromium and alumina. as the sintering temperature is increased (1000 and 1100°C), the peaks for the sample are matched with the standard. It is believed that, during sintering process at 900°C, the phases of chromium and alumina was not completely formed yet due to incomplete decomposition of the precursor used to produce alumina doped with chromium[21-23]. However, as the sintering temperature increased to 1000°C, the decomposition of precursor increased and lead to the formation chromium doped alumina phase [22]. Based on the XRD analysis, the crystalline phase of chromium doped alumina begins to appear at higher temperatures (1000 and 1100 °C), while at the lower temperature (900 °C) the amorphous phase dominates, as clearly shown in Fig. 2. The numerous peaks observed in the spectra of the samples sintered at higher temperatures clearly indicate the formation of the crystalline phase of chromium doped alumina. The observation of γ-alumina at 900°C indicates that the transition temperature has not been reached. Whereas, the detected α-alumina in the samples sintered at 1000-1100°C indicates a temperature-driven phase transition ($\gamma \rightarrow \alpha$) and the formation of a stable aluminum chromium oxide ($AlCrO_3$ or $Al_{1.98}Cr_{0.02}O_3$) at higher temperatures due to chromium incorporation into the lattice.

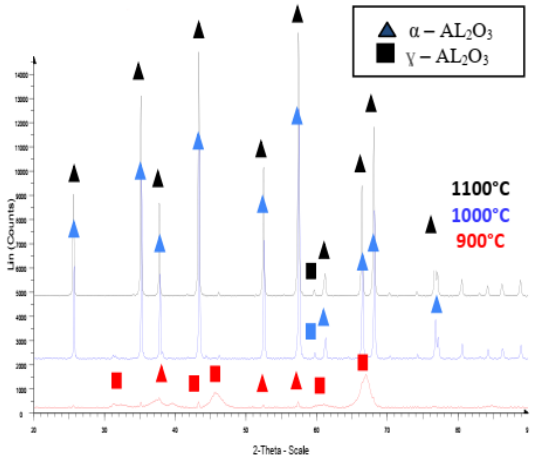

Fig 2. XRD diffractogram for chromium doped-alumina sintered at 900°C (red), 1000°C (blue) and 1100°C (black).

3.2 Field Emission Scanning Electron Microscope (FESEM)

The figures below (i.e., Fig 3., Fig. 4., and Fig. 5) show SEM micrographs for chromium doped alumina sample sintered at various temperatures, with magnification of 500 X and 10000 X. At the magnifications of 500 X, the

particle size of all chromium doped alumina powder samples with different sintering temperatures are observed. The particles of all three samples have similar sizes of several microns (from the scale), averaging at 10µm. The distribution of sizes are obtained as a result of the grinding process. When the magnification is increased to 10000 X, no porosity is observed on the sample sintered at 900°C. This shows that no or little reaction took place in the powder sample due to the low calcination temperature. Thus, there is no combustion happening at 900°C. As for the samples sintered at 1000°C and 1100°C, porosities can be observed in the circled regions in Figure 3(b) and 4(b). The presence of these pores is due to the reaction between carbon (from sugar, $C_{12}H_{22}O_{11}$) and oxygen to give off carbon dioxide. The gaseous carbon dioxide leaves the surface thus pores are formed. However, the amounts of porosity for both samples are small. The most notable difference of samples sintered at 1000°C and 1100°C are the pore size. Sintering at 1100°C produces qualitatively smaller pores than those of 1000°C. It is believed that, as the sintering temperature is increased, the porosity of the sample is decreased as a result of particle fusion[24].

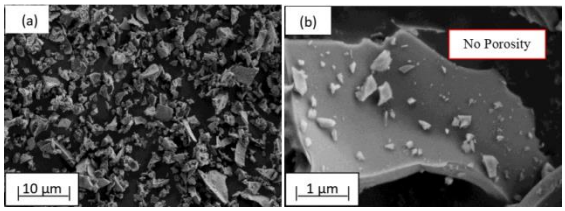

Fig 3. SEM micrographs of chromium doped alumina powder sample sintered at 900°C at magnification (a) 500 X (b) 10000 X.

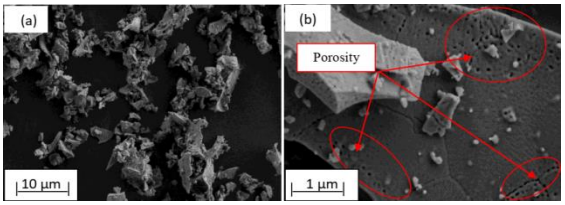

Fig 4. SEM micrographs of chromium doped alumina powder sample sintered at 1000°C at magnification (a) 500 X (b) 10000 X.

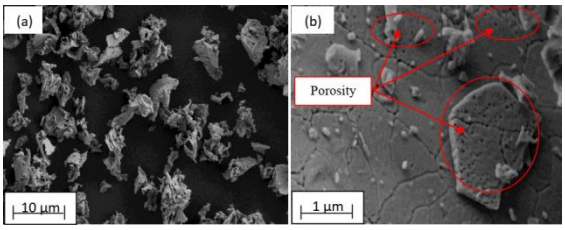

Fig 5. SEM micrographs of chromium doped alumina powder sample sintered at 1100°C at magnification (a) 500 X (b) 10000 X.

3.3 Fourier Transform Infra-Red (FTIR)

Fig. 6 shows the FTIR spectra for samples sintered at 900, 1000 and 1100°C. At wavenumber range of 3843- 3741 cm^{-1}, the same shape of curve was obtained for all three FTIR spectra. This region is believed to be associated with the bonding to the bonding of alcohol that used during the cleaning process of sample preparation[25]. As moving to wavenumber of 2369 cm^{-1}, there are also same peaks obtained for all three spectra. This peak is believed that it belongs to diazonium salts and P-H phospines contamination of the sample. At wavenumber range of 1700-1200 cm^{-1}, peak change is observed for all three spectra. At wavenumber range of 634-441 cm^{-1}, a strong peak is being seen as the sintering temperature is increased. At 900°C, the peak is not clearly visible. This occurs due to the contamination of N-H_3. Compounds containing N-H_3 are known to be volatile or decompose at elevated temperatures. Sintering at 1000 and 1100°C provides more thermal energy and a greater driving force for the complete decomposition and expulsion of these species compared to sintering at 900°C. The complete removal of these residual components at higher temperatures leads to a purer, more homogeneous material with a well-defined crystal structure. [26]. The residual N-H_3 related groups within the sample can act as defects or secondary phases. The samples sintered at 1000 and 1100°C are likely more crystalline due to the more effective removal of the volatile N-H_3 species compared to sample sintered at 900°C. This results in a spectrum with sharper, more

intense characteristic peaks. This increased purity and structural integrity at higher sintering temperatures would naturally lead to a clearer, less complicated spectrum, free from the interference of residual volatile compounds[26-28].

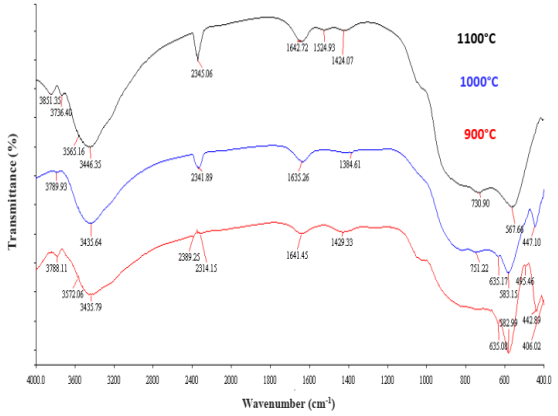

Fig 6. FTIR spectrums for chromium doped alumina sintered at 900°C (red), 1000°C (blue) and 1100°C (black).

4. CONCLUSIONS

The sintering temperature has a strong effect in the formation of chromium doped alumina. High magnification of FESEM showed that, as the temperature increased, the porosity of the sample is decreased due to fusion process occur between the particles. XRD analysis presented that the peaks for chromium and alumina at lower sintering temperature are hardly matched, and as the temperature increased, the peaks are well matched. FTIR analysis showed that there are existences of diazonium, P-H phospines and N-H3 contamination in the samples. Also at wavenumber range of 634-441 cm-1 for all three spectrums, a different transmissions rate is observed. At 900C, the absorption peak is not obvious but as the sintering temperature is increased, the peaks are getting more obvious. based on the currant study, the optimal temperature for the phase formation alumina ceramics is often around 1100°C, but for effective Cr doping, higher temperatures are needed. In conclusion, a higher sintering temperature of at least 1400°C-1600°C is most likely necessary to ensure the complete formation of the desired chromium-doped alumina single phase.

5. ACKNOWLEDGMENT

The author expresses his deepest gratitude for every one who supported this study.

REFERENCES

[1] Adu E, Patel SA, Catino AJ, Medhi R. Polymeric nanoparticles (PNPs) as drug delivery systems for SARS-CoV-2. Characterization and Application of Nanomaterials. 2024;7(1):4959. doi:10.24294/can.v7i1.4959.

[2] Altammar KA. A review on nanoparticles: characteristics, synthesis, applications, and challenges. Front Microbiol. 2023;14:1155622. doi:10.3389/fmicb.2023.1155622.

[3] Kumar K, Chowdhury A. Reviewing the cases of nanoscale heterogeneity in ceramics: boon or bane? Materialia. 2021;16:101109. doi:10.1016/j.mtla.2021.101109.

[4] Vunain E, Mishra S, Mishra AK, Mamba B. Nanoceramics: fundamentals and advanced perspectives. In: Sol-gel based nanoceramic materials: preparation, properties and applications. 2017. p. 1–20. doi:10.1007/978-3-319-49512-5_1.

[5] Wu Q, Miao WS, Zhang YD, Gao HJ, Hui D. Mechanical properties of nanomaterials: a review. Nanotechnol Rev. 2020;9(1):259–273. doi:10.1515/ntrev-2020-0021.

[6] Olugbade TO, Lu J. Literature review on the mechanical properties of materials after surface mechanical attrition treatment (SMAT). Nano Mater Sci. 2020;2(1):3–31. doi:10.1016/j.nanoms.2020.04.002.

[7] Norhasri MM, Hamidah M, Fadzil AM. Applications of using nanomaterial in concrete: a review. Constr Build Mater. 2017;133:91–97. doi:10.1016/j.conbuildmat.2016.12.005.

[8] Jamkhande PG, Ghule NW, Bamer AH, Kalaskar MG. Metal nanoparticles synthesis: an overview on methods of preparation, advantages and disadvantages, and applications. J Drug Deliv Sci Technol. 2019;53:101174. doi:10.1016/j.jddst.2019.101174.

[9] Mishra RK, Ha SK, Verma K, Tiwari SK. Recent progress in selected bio-nanomaterials and their engineering applications: an overview. J Sci Adv Mater Devices. 2018;3(3):263–288. doi:10.1016/j.jsamd.2018.05.003.

[10] Oluwasanu AA, Oluwaseun F, Teslim JA, Isaiah TT, Olalekan IA, Chris OA. Scientific applications and prospects of nanomaterials: a multidisciplinary review. Afr J Biotechnol. 2019;18(30):946–961. doi:10.5897/AJB2019.16812.

[11] Santra TS, Mohan L. *Nanomaterials and their biomedical applications*. Springer; 2021.

[12] Salem SS. Application of nano-materials. In: *Haematococcus: biochemistry, biotechnology and biomedical applications*. Springer; 2023. p. 149–163.

[13] Saji VS, Choe HC, Yeung KW. Nanotechnology in biomedical applications: a review. Int J Nano Biomater. 2010;3(2):119–139. doi:10.1504/IJNBM.2010.037801.

[14] Dehchani AJ, Jafari A, Shahi F. Nanogels in biomedical engineering: revolutionizing drug delivery, tissue engineering, and bioimaging. Polym Adv Technol. 2024;35(10):e6595. doi:10.1002/pat.6595.

[15] Foong LK, et al. Applications of nano-materials in diverse dentistry regimes. RSC Adv. 2020;10(26):15430–15460. doi:10.1039/D0RA00762E.

[16] Chethan B, Prasad V, Sunilkumar A, Veena V, Thomas S. Trends in development of nanomaterial-based sensing devices. In: *Recent Developments in Green Electrochemical Sensors*. ACS Publications; 2023. p. 287–305.

[17] Singh SK, Kulkarni PP, Dash D. Biomedical applications of nanomaterials: an overview. In: *Bio-Nanotechnology: A Revolution in Food, Biomedical and Health Sciences*. 2013. p. 1–32. doi:10.1002/9781118451915.ch1.

[18] Einbergs E, et al. Usability of Cr-doped alumina in dosimetry. Ceramics. 2019;2(3):525–535. doi:10.3390/ceramics2030040.

[19] Nguyen DK, Lee H, Kim IT. Synthesis and thermochromic properties of Cr-doped Al_2O_3 for a reversible thermochromic sensor. Materials. 2017;10(5):476. doi:10.3390/ma10050476.

[20] Zhu YL, Liu S, Zhang XK, Xiang Y. Effects of Cr^{3+} concentration on the crystallinity and optical properties of Cr-doped Al_2O_3 powders by solid-state reaction method. In: IOP Conf Ser Mater Sci Eng. 2018;382:022037.

[21] Nforbi LNN. Phase stability analysis of lanthanum-doped alumina during synthesis and sintering. 2010.

[22] Jiao X, Liu Y, Cai X, Wang J, Feng P. Progress of porous Al-containing intermetallics fabricated by combustion synthesis reactions: a review. J Mater Sci. 2021;56:11605–11630. doi:10.1007/s10853-021-06035-5.

[23] Carofiglio M, Barui S, Cauda V, Laurenti M. Doped zinc oxide nanoparticles: synthesis, characterization and potential use in nanomedicine. Appl Sci. 2020;10(15):5194. doi:10.3390/app10155194.

[24] Sutton AT, Kriewall CS, Leu MC, Newkirk JW. Powder characterisation techniques and effects of powder characteristics on part properties in powder-bed fusion processes. Virtual Phys Prototyp. 2017;12(1):3–29. doi:10.1080/17452759.2016.1250605.

[25] Norby T. Proton conductivity in perovskite oxides. In: Ishihara T, editor. *Perovskite oxide for solid oxide fuel cells*. Boston: Springer; 2009. p. 217–241.

[26] Li J, Pan Y, Xiang C, Ge Q, Guo J. Low temperature synthesis of ultrafine α-Al_2O_3 powder by a simple aqueous sol–gel process. Ceram Int. 2006;32(5):587–591. doi:10.1016/j.ceramint.2005.04.015.

[27] Lee JS, Kim HS, Park NK, Lee TJ, Kang M. Low temperature synthesis of α-alumina from aluminum hydroxide hydrothermally synthesized using [Al(C_2O_4)x(OH)y] complexes. Chem Eng J. 2013;230:351–360. doi:10.1016/j.cej.2013.06.099.

[28] Shao Z, Zhou W, Zhu Z. Advanced synthesis of materials for intermediate-temperature solid oxide fuel cells. Prog Mater Sci. 2012;57(4):804–874. doi:10.1016/j.pmatsci.2011.08.002.